



Treball Final de Grau

Organometallic chemistry with phosphines presenting unconventional coordination modes.

Química organometàl·lica amb fosfines que presenten modes de coordinació poc convencionals.

Sara Torrente Gómez

Juny 2019



UNIVERSITAT DE
BARCELONA

B:KC Barcelona
Knowledge
Campus
Campus d'Excel·lència Internacional

Aquesta obra esta subjecta a la llicència de:
Reconeixement–NoComercial–SenseObraDerivada



<http://creativecommons.org/licenses/by-nc-nd/3.0/es/>

Y, sin embargo, se mueve.

Galileo Galilei

Volia donar les gràcies, en primer lloc, als meus pares, ja que sense ells jo no hi seria ni hauria arribat fins aquí. No m'oblido del Marc, que encara que potser ell no se n'adoni, també fa coses per mi i es fa estimar. Sento haver estat tan desagradable a casa alguns dies d'estrès, no m'ho tingueu gaire en compte. Gràcies també a la resta de la família.

Agrair als membres de "El club de la petanca", als que hi són i al que ens va deixar, els bons moments i el fer que estigui envoltada de gent meravellosa que m'estima, i a la que estimo. D'entre ells, destacar la meva segona família: el Pepe, l'Esperanza, l'Ana i la María.

Donar les gràcies també a la Paula, per aguantar-me aquests cinc anys de carrera, malgrat que la situació no és gens fàcil.

Gràcies als meus amics, als de sempre i als nous. Mil gràcies per tot Elis, Anna i Adriana.

Agrair a tothom del laboratori del grup de Catàlisi Homogènia l'acollida, el bon ambient, els riures i l'ajuda d'aquests mesos. Sense oblidar-me del grup del cafè de les 8:15, que em feia començar el dia amb riures i energia.

I per últim, moltíssimes gràcies al Dr. Arnald Grabulosa per descobrir-me aquesta química tan maca, bruta i addictiva alhora, com ho és la del fòsfor. Espero que la puguis continuar fent i ensenyant molts més anys.

REPORT

CONTENTS

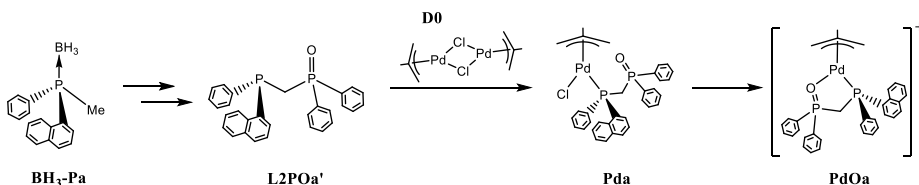
1. SUMMARY	3
2. RESUM	5
3. INTRODUCTION	7
4. OBJECTIVES	10
5. RESULTS AND DISCUSSION	11
5.1. Synthesis of [Pd(η^3-2-methylallyl)(P*RR'CH₂POR₂-κ^2P*,O)] complexes	11
5.1.1. Preparation of BH ₃ -P*P(O) ligands	11
5.1.2. Deprotection of BH ₃ -P*P(O) ligands	13
5.1.3. Synthesis of κ^1 P*-palladium complexes	15
5.1.4. Obtention of the κ^2 P*,O-palladium complexes	16
5.2. Synthesis of [RuCl₂(η^6-arene)(P(PhPyr)R₂)] complexes	17
5.2.1. Preparation of 1-(2-pyrenyl)phenyl phosphines	18
5.2.2. Synthesis of ruthenium complexes	18
5.2.3. Obtention of the tethered ruthenium complexes	22
6. EXPERIMENTAL SECTION	25
6.1. Materials and methods	25
6.2. Characterisation of the products	25
6.3. Chiral, partial and selectively mono-oxidized diphosphine ligands	26
6.3.1. L2POa	26
6.3.2. L2POa'	27
6.4. Synthesis of palladium complexes containing the L2POa' ligand	27
6.4.1. Pda	27
6.4.2. PdOa	28
6.5. Preparation of 1-(2-pyrenyl)phenyl phosphines	29
6.5.1. PhPyr-Br	29
6.5.2. PaPhPyr	30

6.5.3. PbPhPyr	30
6.6. Synthesis of ruthenium complexes containing the 1-(2-pyrenyl)phenyl phosphines	31
6.6.1. Ru1a	31
6.6.2. Ru2a	32
6.6.3. Rua'	33
6.6.4. Ru1b	33
6.6.5. Ru2b	34
6.6.6. Rub'	34
7. CONCLUSIONS	35
8. REFERENCES AND NOTES	37
9. ACRONYMS	39
APPENDICES	41
Appendix 1: NMR spectra	43

1. SUMMARY

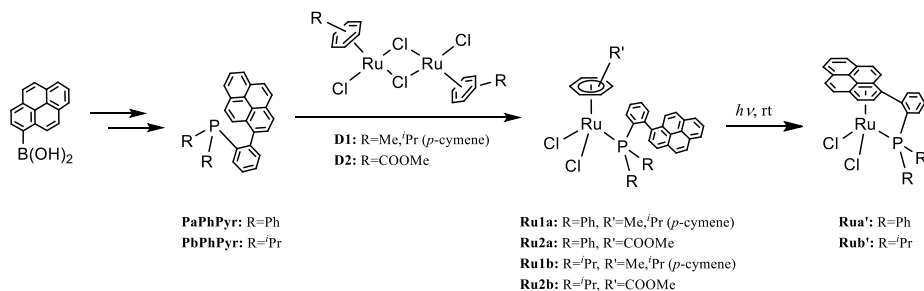
In this work, two differentiated blocks about the synthesis of complexes containing phosphine ligands presenting unconventional coordination modes are described.

Following and adapting methods from literature, chelated palladium(II) complexes with general formula $[\text{Pd}(\eta^3\text{-2-methylallyl})(\text{P}^*\text{RR}'\text{CH}_2\text{POR}_2\text{-}\kappa^2\text{P}^*,\text{O})](\text{PF}_6)$ were synthesized. Starting from $\text{BH}_3\text{-Pa}$, a *P*-stereogenic phosphine, chiral mono-oxidized diphosphine ligands were prepared and subsequently coordinated to Pd(II) centres by the splitting of a dimer complex of Pd(II), **D0**, resulting in two isomers of **Pda**. The corresponding chelated complexes were obtained from **Pda**, using halide scavengers to force the $\text{P}^*\text{P}(\text{O})$ ligand to act as a bidentate, resulting in a five-membered ring metallocyclic cationic complexes, **PdOa**, which also presented two isomers.



The synthesized ligands and complexes were characterized by ^{31}P , $^{31}\text{P}\{^1\text{H}\}$ and ^1H NMR.

In the second part, the synthesis of four ruthenium complexes with general formula $[\text{RuCl}_2(\eta^6\text{-arene})(\text{P}(\text{PhPyr})\text{R}_2)]$ and their derived two tethered complexes are described. 1-pyrenyl boronic acid was used as starting material to synthesize two phosphine ligands, **PaPhPyr** and **PbPhPyr**, which were coordinated to ruthenium centres by the splitting of two different metallic precursors, **D1** and **D2**, obtaining **Ru1a**, **Ru2a**, **Ru1b** and **Ru2b**. Later, the corresponding tethered complexes were prepared under mild conditions by means of photochemical processes when they were just exposed to light of a common office lamp at room temperature, obtaining **Rua'** and **Rub'**.



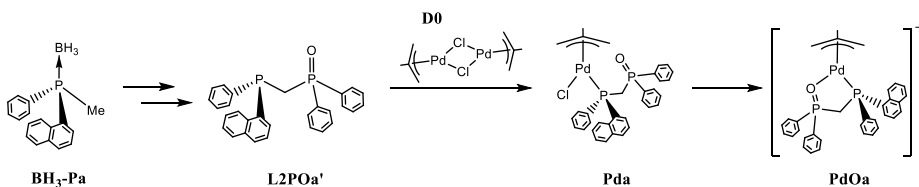
The ligands and the complexes were characterized by ^{31}P , ^{31}P { ^1H }, ^1H , ^{13}C and ^{13}C - ^1H gHSQC NMR, EA and HRMS, and also by XRD when it was possible.

Keywords: Chiral diposphines, palladium complexes, palladium metallocycles, phosphine oxides, pyrenyl phosphines, ruthenium complexes, tethered complexes, organometallics, bioorganometallic chemistry.

2. RESUM

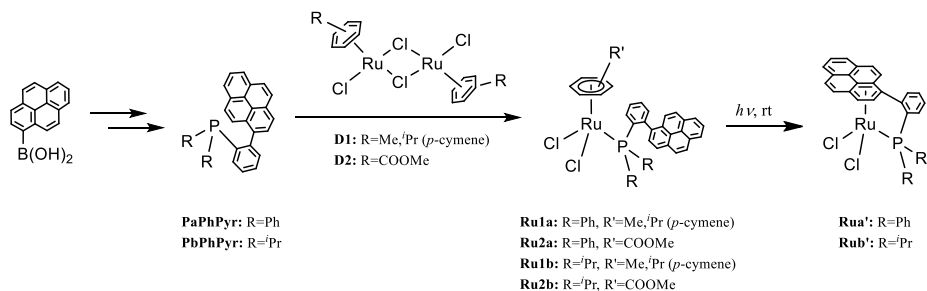
En aquest treball, es descriu, en dos grans blocs diferenciats, la síntesi de complexos que contenen diferents lligands difosfina que presenten modes de coordinació poc convencionals.

Seguint i adaptant mètodes de la bibliografia, es van sintetitzar complexos quelats de pal·ladi(II) amb fórmula general $[\text{Pd}(\eta^3\text{-2-metilal·lil})(\text{P}^*\text{RR}'\text{CH}_2\text{POR}_2\text{-}\kappa^2\text{P}^*,\text{O})](\text{PF}_6)$. Començant per **BH₃-Pa**, una fosfina *P*-estereogènica, es van preparar lligands difosfina quirals i mono-oxidats que es van coordinar a nuclis de Pd(II), mitjançant la reacció amb un complex dímer de pal·ladi(II), **D0**, obtenint dos isòmers de **Pda**. Posteriorment, **Pda** es va tractar per eliminar el lligand clorur de l'esfera de coordinació del metall, forçant, així, que el lligand P*P(O) actués com a bidentat, donant lloc a un compost catiònic metal·locíclic de cinc baules, **PdOa**, que també presenta dos isòmers.



Els lligands i els complexos sintetitzats es van caracteritzar mitjançant ^{31}P , $^{31}\text{P}\{^1\text{H}\}$ i ^1H NMR.

A la segona part, es presenten la síntesi i la caracterització de quatre complexos de ruteni amb fórmula general $[\text{RuCl}_2(\eta^6\text{-arè})(\text{P}(\text{PhPyr})\text{R}_2)]$, i el seu posterior tancament per obtenir dos nous complexos. Fent servir àcid 1-pirenilborònic com a reactiu de partida, es van preparar dos lligands fosfina, **PaPhPyr** i **PbPhPyr**, que es van coordinar a centres de ruteni a partir de la reacció amb dos precursors metàl·lics diferents, **D1** i **D2**; obtenint els complexos mononuclears **Ru1a**, **Ru2a**, **Ru1b** i **Ru2b**. A continuació, els corresponents complexos tancats es van preparar a partir dels anteriors, en condicions suaus, mitjançant processos fotoquímics, exposant-los a la llum d'una làmpada d'oficina a temperatura ambient, obtenint **Rua'** i **Rub'**.



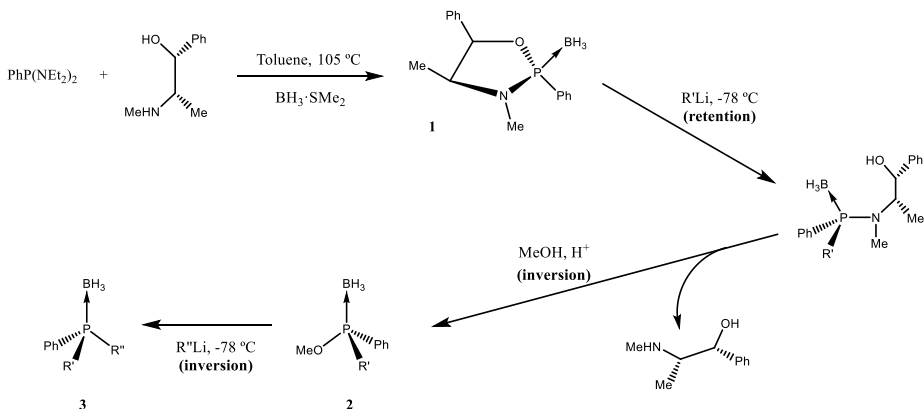
Els lligands i els complexos es van caracteritzar mitjançant ^{31}P , $^{31}\text{P} \{^1\text{H}\}$, ^1H , ^{13}C i ^1H - ^{13}C gHSQC NMR, EA i HRMS, i també mitjançant XRD quan va ser possible.

Paraules clau: difosfines quirals, complexos de pal·ladi, metal·locicles de pal·ladi, monòxid de difosfina, pirenilfosfines, complexos de ruteni, complexos, química organometàl·lica, química bio-organometàl·lica.

3. INTRODUCTION

Phosphines are very common compounds used as ligands in coordination chemistry and homogeneous catalysis. Thanks to the differentiated properties because of the substituents in the phosphine ligands, complexes containing phosphines can be used in so many fields. The group of *Catàlisi Homogènia* of the *Universitat de Barcelona* is an example of the phosphines' versatility, as it can be seen due to the two well differentiated parts in this work.

One of the most important applications is in homogeneous asymmetric catalysis, field in which the group has worked with several types of chiral phosphines and derivatives. The synthesis *P*-stereogenic ligands is carried out following the Jugé-Stephan method, shown in Scheme 1, using the aminoalcohol ephedrine as a chiral auxiliary^[1].



Scheme 1. Jugé-Stephan method for the obtention of *P*-stereogenic phosphines.

The first step of this method is the formation of an enantiopure oxazaphospholine-borane (Scheme 1, **1**), by means of the stereoselective cycling of ephedrine with the initial phosphine, obtaining the R_P diastereomer because of the high steric hindrance when it is S_P . The borane group, apart from preventing the product oxidation, is needed to ensure the stereoselectivity of the subsequent reactions.

Then, by the addition of the first organolithium reagent, the P-O bond is regio- and stereoselectively opened, with retention of the configuration at the phosphorus centre. In this step, 1-naphthyl group was introduced to the obtain the phosphines used in this work.

A later acidic methanolysis, occurring by a S_N2 reaction, with inversion of configuration, yields the phosphinite-boranes (Scheme 1, **2**).

Finally, a second addition of organolithium reagent is carried out and, the methoxy group is substituted in a S_N2 reaction, in our case by a methyl group. The chiral phosphine-borane (Scheme 1, **3**) is obtained pure with S_P configuration.

Currently, the group is focused in developing chiral methylene bridge diphosphine ligands^[2] (Figure 1, **4**), using the chiral P(Me)PhR, prepared by Jugé-Stephan method, and achiral chlorophosphines. This ligands are then coordinated to Pd centres in order to synthesize complexes with general formula $[PdX_2(PR_2CH_2P^*PhR')]$, presenting different combinations of alkyl and aryl substituents (isopropyl, phenyl, 1-naphthyl, biphenyl...) and with X = anionic ligand. It allows to study the influence of the catalytic activity and selectivity depending on the phosphine properties.

Related to diphosphine ligands, phosphine oxides or diphosphine dioxides acting as bidentate ligands are also common ligands for transition metals such as La, Nd, Pm, Sd and Eu (Figure 1, **5**).^[3]

In this work, the synthesis of P*P(O) methylene bridge ligands, combining both previously mentioned diphosphine ligands, is described. The later coordination to Pd centres, and the catalytic tests will determine their catalytic activity and enantioselectivity, in order to discover how the oxide affects. There are a few examples in the literature^[4], (Figure 1, **6**) but the novelty of ours lies in the fact that they present a *P*-stereogenic centre while all the reported do not.

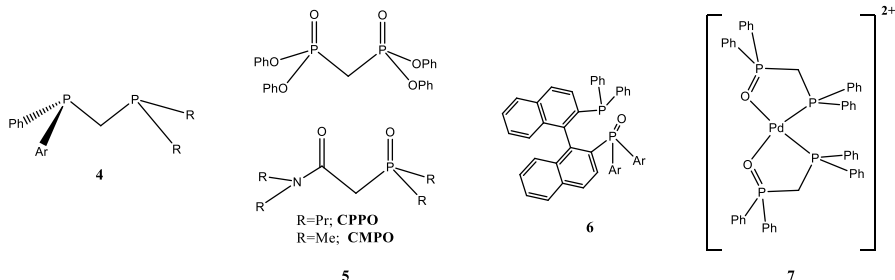


Figure 1. Examples of diphosphines developed in the group (**4**), and phosphine and diphosphine oxides (**5**, **6**) and metalocycles from literature (**7**).

After the obtention of the Pd complexes, we will go one step further, trying to obtain the chelated ones, forcing the phosphine ligands to act as bidentate, expecting a coordination via (P*,O) and obtaining cationic five-membered metallocyclic Pd(II) complexes. There are a few examples on the literature^[5] (Figure 1, 7) but none of them contain chiral methylene bridge phosphines.

Also, other previous studies of the group were focused on the synthesis of Ru complexes with general formula $[\text{RuCl}_2(\eta^6\text{-arene})(\text{PR}_3)]$, with R being a *P*-stereogenic phosphine. When Ru metallodrugs started to be developed because of their advantages (similar antitumoral activity, antimetastatic properties and better selectivity towards cancer cells) compared palladium ones, which presented severe side effects. That was the reason why, when the similarity of the complexes of the group with RAPTA family Ru metallodrugs was seen (Figure 2), cytotoxic tests were carried out. The results concluded that, of all of them, complexes containing phosphines with the 1-pyrenyl substituent presented the highest antitumoral activity^[6]. That was the reason why a second generation of ruthenium metallodrugs based on chiral 1-pyrenyl phosphines, $[\text{RuCl}_2(\eta^6\text{-arene})(\text{PPyR}'\text{R}'')]$, was developed (Figure 2). In that line of cytotoxic tests, it was found that the more hindered the phosphine, the lowest antitumoral activity and, also that *p*-cymene compounds were less active than the methyl benzoate analogues.

Combining the results obtained from the second generation and the found in literature, that changing chloride by iodide in ruthenium complexes produced more cytotoxic systems^[7], a third generation of metallodrugs, based on both 1-pyrenyl group and iodide (Figure 2), with general formula $[\text{RuI}_2(\eta^6\text{-arene})(\text{PPyR}_2)]$ was prepared to test their antitumoral effect.

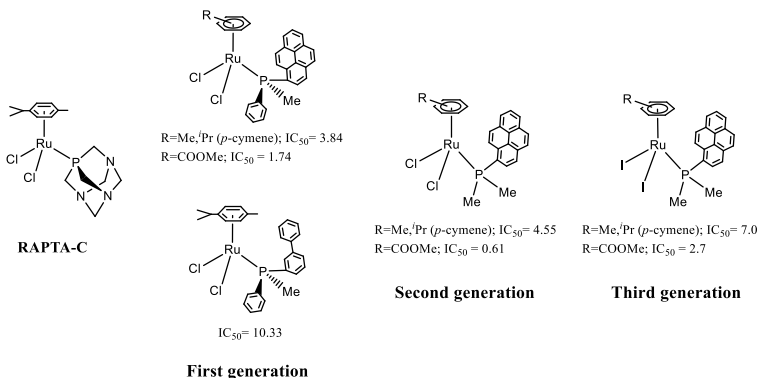


Figure 2. Examples of the evolution of Ru metallodrugs prepared in the group and their IC_{50} values (μM) against SW620 (human colon carcinoma) cell line.

At this point, it was considered that a possible improvement would be the insertion of the metallodrugs into DNA. That is the reason which aims to produce a fourth generation of these ruthenium metallodrugs. It could be that having the 1-pyrenyl group as a substituent in a phenyl group coordinated to the phosphine, instead of directly bonded to it, reduces the hindrance of the compound to 1-pyrene, facilitating its insertion in DNA thanks to π - π stacking interactions with the nitrogenous bases. The results for cytotoxic tests will answer this question.

This project describes the work carried out on this fourth generation of ruthenium metallodrugs with the novelty of the attempt of tethering this ruthenium metallodrugs with the 1-pyrenyl group, like did before in several studies for other aryl ligands^[6,8a,8b], in order to study if it has a repercussion on their antitumoral activity.

4. OBJECTIVES

- Synthesis and characterization of chiral, mono-oxidized methylene bridge diphosphine ligands, P*P(O).
- Synthesis and characterization of palladium(II) complexes with general formula $[\text{Pd}(\eta^3\text{-2-methylallyl})(\text{P}^*\text{RR}'\text{CH}_2\text{POR}_2\text{-}\kappa^2\text{P}^*,\text{O})](\text{PF}_6)$, containing the P*P(O) ligands acting as chelating.
- Synthesis and characterization of **PaPhPyr** and **PbPhPyr**, phosphine ligands containing the 1-(2-pyrenyl)phenyl substituent.
- Synthesis and characterization of ruthenium complexes with general formula $[\text{RuCl}_2(\eta^6\text{-arene})(\text{P}(\text{PhPyr})\text{R}_2)]$ and their corresponding tethered complexes resulting from photochemical processes in which the arene is decoordinated.

5. RESULTS AND DISCUSSION

5.1. SYNTHESIS OF $[\text{Pd}(\eta^3\text{-2-METHYLALLYL})(\text{P}^*\text{RR}'\text{CH}_2\text{POR}_2\text{-}\kappa^2\text{-P}^*,\text{O})]$ COMPLEXES

In this first part of the work, the synthesis of a chiral diphosphine ligand and preliminary coordination studies to Pd(II) were carried out with the objective to ascertain whether the diphosphine ligand could act as a bidentate and chelating one, coordinated via (P*,O). Figure 3 shows the non-chelated and the chelated Pd(II) complexes.

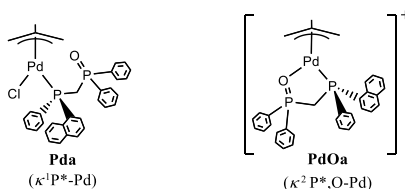
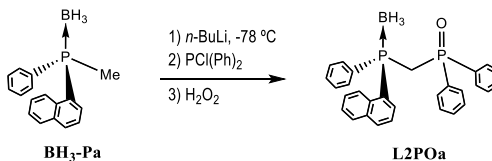


Figure 3. Structures of Pd complexes with **L2POa** as mono (left) and bidentate (right) ligand.

5.1.1. Preparation of $\text{BH}_3\text{-P}^*\text{P}(\text{O})$ ligands

The first experiment consisted in obtaining the mono-oxidized diphosphine-borane ligand, **L2POa**, by the deprotonation of **BH₃-Pa** in tetrahydrofuran using *n*-BuLi, the later phosphination with chlorodiphenylphosphine^[2] and, finally, the oxidation by means of hydrogen peroxide, as shown in Scheme 2.



Scheme 2. *Method A* for the obtention of **L2POa** protected ligand.

Once the workup was finished, the crude was analysed by $^{31}\text{P}\{^1\text{H}\}$ NMR. The spectrum showed, both major, a doublet at 23.8 ppm, with $J_{\text{PP}}=14.1$ Hz, and a broad signal at 15.5 ppm. As expected, the most highly shielded peak was a doublet, due to the coupling of the two phosphorous atoms in the compound, belonging to the oxidized phosphorous, the less shielded one. On the other hand, the broad signal corresponded to the borane-protected phosphorus,

and it was broad due to the effect of the boron quadrupolar moment in the coupling. There were also some other minor peaks at typical chemical shifts for phosphine hydrolysis and oxidation products and, some peaks pertaining to the starting material, **BH₃-Pa**.

It was necessary to purify the product, but since there were not many examples of this type of ligands in the literature to compare the different options to purify the product, several recrystallisation tests were done to find the optimal combination of solvents. Finally, **L2POa** was recrystallised from ethyl acetate and hexane. The white solid, whose $^{31}\text{P}\{^1\text{H}\}$ NMR spectra (Figure 4) showed only the two major signals mentioned before at 24.1 and 15.6 ppm, was obtained pure but, unfortunately, in very low yield.

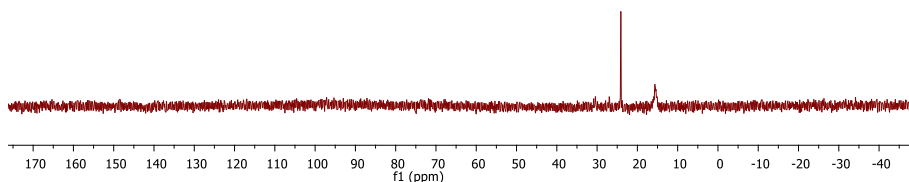


Figure 4. $^{31}\text{P}\{^1\text{H}\}$ spectrum of pure **L2POa**.

Regarding the ^1H NMR spectrum, between 7-8.5 ppm the signals belonging to the aromatic protons were found. In the aliphatic region, two differentiated multiplets were expected for each one of the bridge protons, resulting of the coupling of each one of them with both phosphorous nucleus and the not considered proton of the bridge, because they are not equivalent due to the chirality of one of the phosphorus atoms. Instead of that, about 3.5 ppm a set of different peaks complicated to analyse was recorded. Anyway, the integration of those unexpected signals and the aromatic ones matched with those expected. It could also be mentioned the very low intensity broad centred around 1.15 ppm due to the protons in the borane group.

Data from HRMS matched those calculated, which confirmed the idea that the obtained compound really was **L2POa**.

Since after multiple experiments the desired product could not be obtained again as a pure solid, it was clear the method was not convenient. So, another synthesis strategy was explored.

The second and last one attempt to obtain **L2POa** as a pure solid was carried out following *Method B*, consisting in the deprotonation of **BH₃-Pa** with *n*-BuLi and the addition of the chlorodiphenylphosphine oxide to avoid one of the considered critical steps of the synthesis, which was the oxidation of the previously obtained diphosphine-borane.

The results obtained by this second method were not much better than those obtained by *Method A*, the resulting product was also contaminated with some oxidation and hydrolysis products which could not be removed by recrystallisation. The low yields and the impurity of the obtained solids in the different experiments carried out following the two mentioned methods did not allow the full characterisation of the pure product, for that reason no more ligands were synthesized. Pending job for the future will be to optimise the synthesis procedure.

5.1.2. Deprotection of $\text{BH}_3\text{-P}^*\text{P}(\text{O})$ ligands

In order to synthesize the Pd complexes, the deprotection of the obtained ligands and the elimination of all the borane from the medium were crucial steps. Sometimes the complexes can be obtained from the borane-phosphine adduct, but it was not the case since the reduction of $\text{Pd}(\text{II})$ to $\text{Pd}(0)$ occurs easily in presence of any reducing agent.

Two different methods were simultaneously carried out to deprotect **BH₃-Pa**. For arylphosphine-borane adducts deprotection, *Method A*^[8a], using a secondary amine as morpholine or diethylamine is common, but its effectiveness was not assured for the ligands we were working with because of the presence of the oxide. For this reason, *Method B*^[8a], which was considered more aggressive and probably more effective, usually used in case of trialkylphosphine-boranes deprotection using a strong acid with a weakly coordinating, nonoxidizing conjugate base, such as tetrafluoro boric acid diethyl ether complex, and the subsequent neutralization with sodium hydrogen carbonate, was also carried out.

In that experiment, **L2POa**'s crude was dissolved in 10 mL of dichloromethane and the resulting solution was divided in two 5 mL volume fractions. Afterwards, the solvent was removed under vacuum in both fractions.

The mono-oxidized diphosphine-borane, **L2POa**, from one of those fractions was deprotected following *Method A*, using 5 mL of morpholine, and the morpholine solution was analysed by $^{31}\text{P}\{^1\text{H}\}$ inset NMR. The inset consisted in a self-made coaxial NMR tube containing $\text{P}(\text{OMe})_3$ as a reference substance, dissolved in C_6D_6 . The advantage of recording this type of NMR spectra is that a reaction can be easily monitored just taking a crude's aliquot, without doing the work up and dissolving the product in deuterated solvents. It saves time, work and product.

The complete deprotection was confirmed by the fact the signals corresponding to **L2POa** (15.6 and 24.1 ppm) disappeared and new peaks belonging to the free ligand **L2POa'** appeared at -38.6 and 26.7 ppm, belonging to the free and the oxidized phosphorus nuclei, respectively. As expected, the oxidized phosphorous chemical shifts did not change significantly between both species, but the one of the deprotected phosphorous moved to lower chemical shifts in case of **L2POa'** due to the lower shielding compared to **L2POa**. Also, a minor signal corresponding to **Pa** was found at -38.3 ppm.^[9a]

After the purification by chromatography column (Al_2O_3 , toluene), the $^{31}\text{P}\{^1\text{H}\}$ NMR spectrum was recorded. Surprisingly, the spectrum showed only the singlet of **Pa**. As we could see, *Method A* did not allow the obtention of the pure free ligand because the product was retained in the stationary phase, probably because of its polarity due to the presence of the oxide. For the future, a possible solution could be the purification by chromatography column using basic silica and other eluents.

For the deprotection of **L2POa** by *Method B*, the remaining fraction was dissolved in 5 mL of dichloromethane and the mixture was cooled down to 0 °C. Subsequently, the tetrafluoro boric acid diethyl ether complex was added, and the mixture was left stirred for 1 h. After that time, the $^{31}\text{P}\{^1\text{H}\}$ and ^{31}P inset NMR spectra of the phosphonium salt were recorded in order to check if the process was completed (Appendix 1, **1** and **2**).

As expected, the signals belonging to **L2POa** (15.6 and 24.1 ppm) disappeared in both spectra and new peaks belonging to the phosphonium salt appeared. In case of $^{31}\text{P}\{^1\text{H}\}$ spectrum, two broad singlets centred at 44.4 ppm and -2.8 ppm were found, corresponding to the oxidized phosphorus and the free one, respectively. Not as expected, it seemed the oxide was also protonated, since due to the lower shielding its chemical shift was higher than the typical for oxidized phosphorus. Also, a signal at -4.7 ppm, pertaining to the phosphonium salt of **Pa**, was found. In the ^{31}P NMR spectrum the same two signals were observed, but in that case, the one centred -2.8 ppm was a doublet with a large J of 517.3 Hz, typical of P-H moieties, whose fine structure could be appreciated as quintuplets due to the coupling of the phosphorus atom with four protons.

Once the complete deprotection was confirmed, the phosphonium solution was neutralized with NaHCO_3 , and extracted under nitrogen with dichloromethane to isolate the neutral free $\text{P}^*\text{P}(\text{O})$ ligand in the organic phase. The final product was analysed by $^{31}\text{P}\{^1\text{H}\}$ NMR.

The signals corresponding to the phosphonium salt disappeared and new peaks belonging to the free ligand **L2POa'** appeared as two sharp doublets at -37.1 and 25.3 ppm, being assignable to the free and the oxidized phosphorous centres, respectively (Appendix 1, 3).

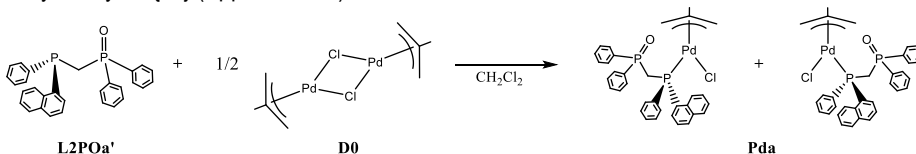
The differences observed between the chemical shifts obtained for the phosphorous nuclei in both experiments following the two different methods (26.7 vs. 25.3 ppm and -38.6 vs. -37.1 ppm) could be due to the fact the $^{31}\text{P}\{^1\text{H}\}$ NMR spectra were recorded by two different instruments, since the measured coupling constant for P-P coupling was around 53.5 Hz in both cases.

Other interesting data to compare are the coupling constants for P-P coupling in the protected and the deprotected diphosphine, in case of **L2POa** J_{PP} was around 14.1 Hz whereas for **L2POa'** it was around 53.5 Hz. As it usually happens, the coupling constant J_{PP} increases when the borane is removed, as in reported cases^[8a].

In both cases, the deprotection took place but, in case of *Method B* we could see the deprotection was complete after 1 h stirring while, in case of *Method A*, it took around 24 h. Besides, the product only could be obtained separated from borane following *Method B*, since the purification by chromatography column to remove the morpholine-borane in case of *Method A* did not work. So, it seems *Method B* is faster and more adequate for our P*P(O) ligands.

5.1.3. Synthesis of $\kappa^1\text{P}^*$ -palladium complexes

To obtain the desired palladium complexes, the free ligand **L2POa'** was dissolved in deoxygenated dichloromethane and subsequently, **D0** was added to the resulting solution (Scheme 3).^[6,8a,8b] After 1 h stirring, **Pda**'s crude was obtained as a colourless oil and then, analysed by $^{31}\text{P}\{^1\text{H}\}$ (Appendix 1, 4) and ^1H NMR.



Scheme 3. Preparation of **Pda** by splitting of **D0**. Both possible isomers are showed.

Regarding to $^{31}\text{P}\{^1\text{H}\}$ NMR spectrum of **Pda**, it was expected to find to pairs of major sharp doublets because of the presence of the two isomers of **Pda**, due to the two different diastereomers formed upon dimer splitting^[9a]. Instead of that, the $^{31}\text{P}\{^1\text{H}\}$ NMR spectrum

showed two major sharp doublets at 25.5 and 24.7 ppm, and a signal similar to a triplet around 8.4 ppm because of the superposition of the two similar shifted remaining doublet signals. The two isomers were obtained in 0.62/0.38 ratio. The major one was assigned to the signals at 25.5 and 8.38 ppm while the minor of them was assigned to the 24.7 and 8.42 ppm doublets. Other minor signals with higher chemical shifts, probably corresponding to some oxides, were also found. Thanks to previous works^[9b], two minor signals at 4.9 and 4.6 ppm could be assigned to both $[\text{PdCl}(\text{2-methylallyl})(\text{Pa})]$ isomers, something expected since **L2POa** was impurified with **Pa**.

5.1.4. Synthesis of the $\kappa^2\text{P}^*,\text{O}$ -palladium complexes

The main objective of this part of the work was to obtain these chelate palladium complexes^[4,5,9a] with the $\text{P}^*\text{P}(\text{O})$ ligand in a bidentate coordination type $\text{P}^*-\text{Pd}-\text{O}$ resulting in so stable five membered ring complexes (Figure 3).

Once **Pda** was obtained, it was treated with halide scavengers in order to achieve that mentioned bidentate (P^*,O) coordination mode of the ligand. Two methods, using NH_4PF_6 and TIPF_6 , were simultaneously carried out to decoordinate the chloride ligand from the complex and forcing the $\text{P}^*\text{P}(\text{O})$ ligand to act as a bidentate.

Both methods followed use the same principle, which consists in taking benefit of the difference between the sizes of the anion and the cation of both, the salt we have and another one we are interested to exchange the ions with. In case of TIPF_6 method, the insolubility of TlCl formed facilitates the reaction. The bulkiest ions tend to interact stronger with each other, and vice versa. So, when NH_4PF_6 or TIPF_6 are added to the complex solutions, Cl^- ligand is expected to be more attracted by NH_4^+ or Tl^+ compared to the cationic complex, which, simultaneously, is strongly attracted by PF_6^- anion. This way, we would remove the chloride from the Pd complex, obtaining an electron-deficient non-stable cationic Pd complex and PF_6^- , a non-coordinating anion, as the ions of the new salt. The vacancy left by the chloride anion at the Pd coordination sphere is going to be occupied by our $\text{P}^*\text{P}(\text{O})$ ligand, acting as bidentate.

Regarding TIPF_6 , it was expected to work better than NH_4PF_6 because of the greater difference between the ions in the salt and the greater similarity with the ions of the complex and, basically, due to the insolubility of TlCl . Even so, the two methods were carried out to

check if the results between them were similar, since it was preferable to work with NH_4PF_6 to avoid using TIPF_6 in the future because of its toxicity.

To carry out the experiments, **Pda** was divided in two equal volume fractions, each one treated with one of the two reagents indicated above, and the resulting products were both analysed by $^{31}\text{P}\{^1\text{H}\}$ and ^1H NMR.

In case of *Method A*, using NH_4PF_6 , the major signal in $^{31}\text{P}\{^1\text{H}\}$ NMR spectrum was a singlet around 30 ppm, a typical chemical shift for phosphine oxides. It also seemed to appear four minor doublets, apart from those around 1 and -2 ppm belonging to $[\text{Pd}(\text{2-methylallyl})(\text{Pa})_2](\text{PF}_6)$ impurities, which could correspond to both **PdOa** isomers. As expected, around -144 ppm appeared a quintuplet pertaining to the PF_6^- anion.

The $^{31}\text{P}\{^1\text{H}\}$ NMR spectrum for the resulting product obtained by *Method B* (Appendix 1, 5) showed four signals due to the presence of the two isomers of **PdOa** in solution in ratio 0.60/0.40, two at 60.8 and 15.5 ppm for the major isomer, and other two at 60.3 and 17.2 ppm for the minor one. Like in case of *Method A*, two minor signals corresponding to both isomers of $[\text{Pd}(\text{2-methylallyl})(\text{Pa})_2](\text{PF}_6)$ at 1.1 and -2.1 ppm^[9a], and a quintuplet belonging to the PF_6^- anion around -144 ppm were also found.

According to the results observed in NH_4PF_6 and TIPF_6 cases, *Method B* worked while *Method A* did not work at all. So, despite the toxicity of TIPF_6 it seems a good option to obtain the chelated Pd complexes. Since the products were not obtained pure and in low yields, it did not make sense to do catalytic tests, this will be pending job for the future.

5.2. SYNTHESIS OF $[\text{RuCl}_2(\eta^6\text{-ARENE})(\text{P}(1\text{-(2-Pyr)Ph})\text{R}_2)]$ COMPLEXES

Four ruthenium complexes containing different phosphine and η^6 -arene ligands were synthesised in order to finally obtain two tethered ruthenium complexes (Figure 5).

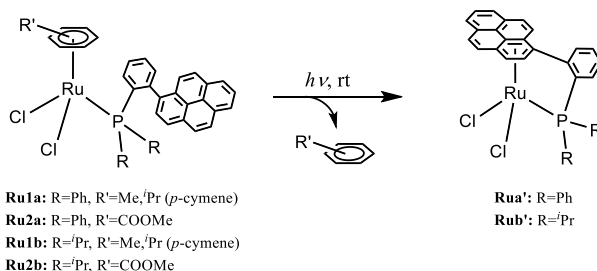


Figure 5. Structures of the Ru complexes.

5.2.1. Preparation of 1-(2-pyrenyl)phenyl phosphines

To obtain the desired complexes, we first needed to prepare the phosphine ligands. 1-bromo-(2-pyrenyl)benzene (**PhPyr-Br**) was synthesized from 1-pyrenyl boronic acid with 1-bromo-2-iodobenzene in 1,2-dimethoxyethane and subjected to a Suzuki-Miyaura coupling using a catalyst of Pd(0). The procedure had been already carried out before in the group to obtain similar phosphine ligands.^[8b,10] After the workup, the product was purified by chromatography column (SiO₂, hexane) and then analysed by ¹H NMR. The characterisation data matched those reported for this compound.^[11]

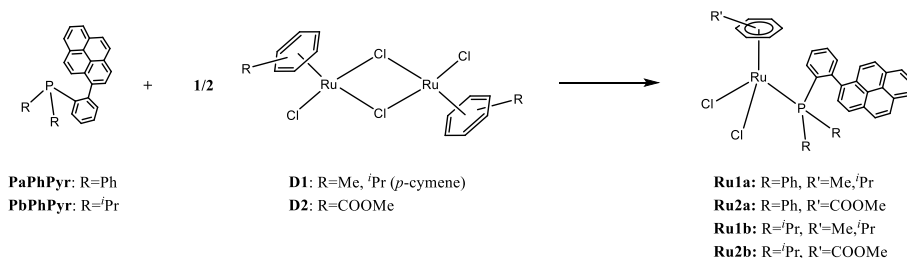
Once **PhPyr-Br** was obtained, **PaPhPyr** and **PbPhPyr** phosphine ligands were prepared by reacting it with chlorodiphenylphosphine, **P-a**, or chlorodiisopropylphosphine, **P-b**, respectively. Both crudes were characterized by ¹H, ³¹P{¹H}, ¹³C{¹H} NMR and gHSQC.

³¹P{¹H} NMR spectrum of **PaPhPyr** showed a major peak at -14.0 ppm whereas the major one for **PbPhPyr** appeared at -4.8 ppm, at higher chemical shifts, as expected. In both cases, the products were not pure, but the impurities were considered minor enough to continue with the synthesis of the complexes.

¹H NMR spectrum of **PaPhPyr** presented only aromatic signals, as expected, since it only has aromatic substituents. In case of **PbPhPyr**, with two isopropyl substituents, it was expected to find the aromatic signals and also the ones corresponding to the isopropyl groups in the aliphatic region, about 1.8 and 0.75 ppm. More signals, due to impurities were also found.

5.2.2. Synthesis of ruthenium complexes

In order to obtain the ruthenium complexes shown in Figure 5, containing the previously prepared **PaPhPyr** and **PbPhPyr** ligands, a method previously carried out in the group^[6,8a,8b], shown in Scheme 4, was followed.



Scheme 4. Obtention of the Ru complexes by dimer precursors splitting.

Ru1a was prepared by mixing **PaPhPyr** and **D1** in dichloromethane for 2 h protected from light. Same way, **Ru2a** was synthesized by mixing **PaPhPyr** and **D2**. In case of **Ru1b** and **Ru2b**, they were obtained by reacting **PbPhPyr** with **D1** and **D2**, respectively. **Ru1a** and **Ru1b** were extracted with water in order to remove any **D1** excess, taking advantage of **D1**'s hydrolysis. In case of **Ru2a** and **Ru2b**, **D2** excess was removed by filtration. Once the workups were finished, all of them were characterised by $^{31}\text{P}\{^1\text{H}\}$ NMR, ^1H NMR, $^{13}\text{C}\{^1\text{H}\}$ NMR, gHSQC, IR, HRMS and EA.

$^{31}\text{P}\{^1\text{H}\}$ NMR spectrum of each complex was expected to show one main signal. So it was for **Ru1a**, **Ru2a** and **Ru1b**, but in case of **Ru2b**, a singlet at 26.9 ppm and a broad peak centred around 50.6 ppm were found in variable ratios between 0.32-0.67/0.68-0.33 in the different experiments (Appendix 1, 6).

Considering all the combinations of the arenes and the phosphine ligands, the most shifted expected complex was **Ru2b**, due to the larger chemical shift of **PbPhPyr** compared to **PaPhPyr** and the presence of the more electron-deficient arene of the two possible, being less important this last mentioned factor. Following the same criteria, in order of most to least shifted, we would have expected: **Ru2b**, **Ru1b**, **Ru2a** and **Ru1a**.

In Table 1 are indicated the chemical shifts found in each case.

Complex	$^{31}\text{P}\{^1\text{H}\}$ shift [ppm]
Ru1a	24.1
Ru2a	26.9
Ru1b	24.1
Ru2b	26.9, 50.6

Table 1. ^{31}P chemical shifts found for ruthenium complexes.

The signals observed in cases of **Ru1a** and **Ru2a** were approximately the expected compared to similar complexes^[6], being able to be appreciated the little difference between the chemical shifts of the complexes due to the coordinated arene in each case, appearing the complex with the methyl benzoate ring at higher shifts. But, not as it was expected, **Ru2a** and **Ru2b** appeared at the same ^{31}P chemical shifts than **Ru1a** and **Ru2a**, respectively. It does not make sense, but according to the results, the most important factor in the variance between the phosphorous chemical shifts in the complexes is the coordinated arene instead of the

phosphine ligand, since **Ru1a** and **Ru2a** $^{31}\text{P}\{^1\text{H}\}$ NMR signals appeared at different chemical shifts whereas **Ru1a** and **Ru1b** showed the same chemical shift value.

Although, for **Ru2b**, the better results obtained for HRMS and EA in cases in which the peak at 50.6 ppm was the major one, made us opt for that signal as the one corresponding to **Ru2b**, it did not make sense that a more shifted signal did not appear also in case of **Ru1b**.

At this point, we considered the possibility that the signals belonging to our complexes were so wide them could not be appreciated, considering then the registered signals belong to impurities in our complexes and not to the complexes themselves. However, the other characterisation data pointed out that the complexes were indeed obtained.

Concerning the ^1H NMR spectra, there were three different regions related to the chemical shifts of the protons in the complexes, as can be seen in Figure 6. The most shifted region was the aromatic one, between 9.5 and 7.0 ppm, followed by the coordinated arene zone, between 6.5 and 4.5 ppm approximately, and finally the aliphatic region, between 4.0 and 0.5 ppm.

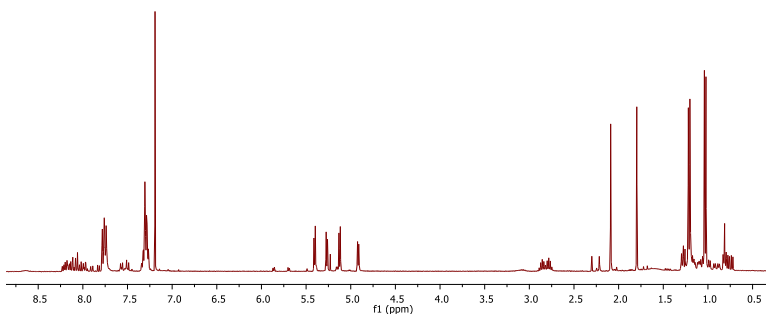


Figure 6. ^1H NMR spectra of **Ru1b**.

According to the registered ^1H NMR spectra, shown in Figure 6, the presence of different rotamers of the complexes seems to be confirmed, since some signals appeared duplicated or even triplicated at different chemical shifts. It could be due to the bulkiness of the arenes, which could not allow the free rotation of the phosphine ligands, making the protons non-equivalent and resulting in more signals than the expected.

One interesting information which could be extracted from IR spectra in case of **Ru2a** and **Ru2b**, the complexes containing the methyl benzoate ring, was the presence of the characteristic $\text{C}=\text{O}$ stretching carbonyl band around 1730 cm^{-1} , confirming the formation of the desired coordination compounds.

Single crystals, suitable for XRD analysis, were obtained for **Ru1a** by diffusion of hexane into a solution of the complex in dichloromethane, which confirmed the obtention of **Ru1a** and, we suppose, all the complexes. Figure 7 shows its molecular structure representation.

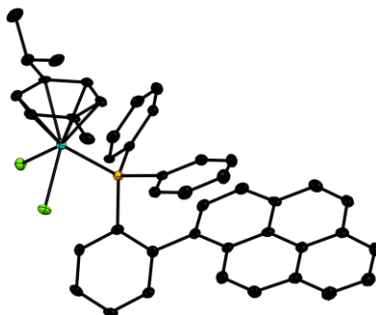


Figure 7. ORTEP representation of **Ru1a** with the thermal ellipsoids drawn at the 50% probability level and hydrogen atoms omitted for clarity.

As expected, the complexes adopt the typical three-legged piano stool geometry for that type of complexes^[8]. The 1-(2-pyrenyl)-phenyl group of the phosphine ligand points outwards the molecule, as for similar reported complexes^[8], maybe due to its bulkiness and the consequent steric effects. Bond distances are in normal ranges for this type of complexes.^[8]

Some interesting metric parameters are listed in Table 2.

Parameter	Ru1a
Ru-Arene _{Center}	1.703
Ru-Cl	2.410
	2.408
Ru-P	2.387
P-C _{Ph}	1.828
	1.821
P-C _{Ph} (PhPyr)	1.850
C _{Ph} (PhPyr)-C _{Pyr}	1.498
Cl-Ru-Cl	89.05
Cl-Ru-P	87.44
	90.64

Table 2. Selected distances (Å) and angles (°) for **Ru1a**.

According to the Ru-ligand distances, it can be seen that distances for the considered legs of the piano-stool structure are similar to each other and larger than this for the centre of the arene, the ligand considered the seat, which is *p*-cymene.

Related to bond distances of the phosphine substituents, the 1-(2-pyrenyl)-phenyl group, shows a larger distance than those for the phenyl ones, with values very close to each other. It is probably due to its greater bulkiness, which causes more steric hindrance than phenyl groups.

Measured angles for Cl-Ru-Cl and Cl-Ru-P are quite lower than 109.5°, fact that allows to confirm the geometry of the Ru centre is not tetrahedral.

5.2.3. Obtention of the tethered ruthenium complexes

Once **Ru1a**, **Ru2a**, **Ru1b** and **Ru2b** were synthesized, it was possible to obtain the tethered Ru complexes, **Rua'** and **Rub'**, under mild conditions by means of photochemical processes when they were just exposed to light of a common office lamp at room temperature.^[8a,8b]

When the η^6 -arenes are coordinated, the Ru nucleus is saturated with 18 valence electrons, but when exposed to light, the coordinated arene decoordinates and the metal centre becomes electron-deficient to be stable. This is the reason why the pyrene group finally coordinates with the Ru centre, recovering the initial 18 electrons around Ru and the corresponding stability.

While **Ru2a** and **Ru2b** were, respectively, completely turned into **Rua'** and **Rub'** in 6 hours, the conversion of **Ru1a** and **Ru1b** into **Rua'** or **Rub'**, respectively, took 4 days. As expected, the *p*-cymene rings were slower decoordinated than methyl benzoates ones, as observed in previous studies of the group.^[8a,8b] It makes sense due to the fact that electron-rich arenes, as *p*-cymene, yield the electrons easier to the metal centre than electron-deficient ones and, as a consequence, the corresponding Ru-arene bond should be stronger in case of electron-rich arenes, thus decreasing the decoordination reaction rate compared to electron-deficient arenes as methyl benzoate.

³¹P{¹H} NMR spectra of **Rua'** and **Rub'** showed in each case a sharp singlet. The signal belonging to **Rua'** was found at 63.1 ppm, as expected, at lower chemical shifts than those for **Rub'**, which appeared at 82.5 ppm (Appendix 1, 7). The chemical shifts are in the expected ranges, according to the literature.^[8a,8b]

When one of the recorded spectra for **Rua'** did not show any signal, the possibility we considered before about the signals we found were those belonging to impurities in our products, and not the products themselves, was reinforced.

However, like in case of the not tethered complexes, the other characterisation data pointed out that the complexes were indeed obtained.

Regarding ^1H NMR spectra, even they did not look very clear because the signals were all broad, the same three regions observed in case of the not tethered complexes were found. As expected, in this case there were less signals in the coordinated arenes zone than in case of the not tethered complexes. It is due to the fact there are only two protons in the coordinated aromatic cycle in case of **Rua'** and **Rub'**; while there are four protons in case of *p*-cymene, in **Ru1a** and **Ru1b**, and five protons in case of methyl benzoate, in **Ru2a** and **Ru2b**.

Regarding to the IR spectra, the disappearance of the characteristic C=O stretching carbonyl band in case of **Rub'**, confirmed the formation of the tethered complex.

Single crystals, suitable for XRD analysis, were obtained for complex **Rub'** by diffusion of hexane into a solution of the complex in dichloromethane. The fact that crystals were obtained, confirmed the obtention of the desired complexes, at least in case of **Ru2b** and **Rub'**, since the solution of **Rub'** which crystallized was obtained by **Ru2b** tethering. Figure 8 shows the molecular structure representation of **Rub'**.

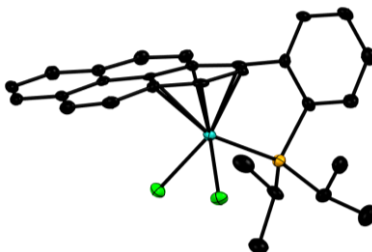


Figure 8. ORTEP representation of **Rub'** with the thermal ellipsoids drawn at the 50% probability level and hydrogen atoms omitted for clarity.

As expected, the tethered complexes still adopt the typical three-legged piano stool geometry but being now the 1-pyrenyl group of the phosphine ligand the one coordinated as the seat of the stool.

In Table 3, some metric parameters are listed.

Parameter	Ru1a
Ru-Arene _{Center}	1.725
Ru-Cl	2.373
	2.397
Ru-P	2.315
P-/Pr	1.844
	1.843
P-C _{Ph(PhPyr)}	1.826
C _{Ph(PhPyr)} -C _{Pyr}	1.490
Cl-Ru-Cl	85.94
Cl-Ru-P	90.94
	93.63

Table 3. Selected distances (Å) and angles (°) for **Rub'**.

According to the Ru-ligand distances listed in Table 3, it can be seen that also for the tethered complex, the distances for the considered legs of the piano-stool structure are similar to each other and larger than this for the centre of the coordinated arene, the ligand considered the seat, which now is the 1-pyrenyl group of the phosphine.

In case of P-R distances in the tethered complex **Rub'**, the P-C_{Ph(PhPyr)} bond shows a shorter distance than those for the isopropyl ones, which present values very close to each other. It is probably due to the greater bulkiness of the isopropyl groups compared to the phenyl one.

Measured angles for Cl-Ru-Cl and Cl-Ru-P are quite lower than 109.5°, like in case of **Ru1a**, the geometry of the Ru centre is neither tetrahedral, as expected.

Distances and angles are in the normal range for this type of complexes, compared to reported similar ones.^[8a,8b]

The fact that crystals could be analysed, confirmed the formation of **Ru1a**, **Rub'** and, as explained before, also the formation of **Ru2b**. So, we supposed all the desired compounds were obtained.

In the future, work concerning higher resolution and variable temperature experiments will be carried out in order to characterize correctly the complexes by ³¹P NMR. Also, cytotoxic tests will be carried out.

6. EXPERIMENTAL SECTION

6.1. MATERIALS AND METHODS

Most of the procedures to obtain the different studied compounds were fully carried out under inert atmosphere, basically, in order to avoid the oxidization of some of the synthesized intermediates or/and products. The used purified nitrogen inert atmosphere was achieved by standard Schlenk and vacuum-line techniques.

The solvents used were obtained from a solvent-purification system or purified by standard procedures and kept under nitrogen.

6.2. CHARACTERISATION OF THE PRODUCTS

^1H , $^{13}\text{C}\{^1\text{H}\}$, $^{31}\text{P}\{^1\text{H}\}$, ^{31}P and gHSQC ^1H - ^{13}C NMR spectra were recorded with 400 MHz spectrometers. The deuterated solvents used to record the NMR spectra are specified in the description of the characterisation of each product. The abbreviations used for the different multiplicities in the studied spectra are: s, singlet; d, doublet; t, triplet; m, multiplet; dd, doublet of doublets; dt, doublet of triplets; bb, broad signal; M, major isomer; m, minor isomer. Regarding to ^1H RMN chemical shifts in **Ru1a**, **Ru2a**, **Ru1b** and **Ru2b** indicated between $[\]$, they refer to the region in which the indicated duplicated signals, corresponding to different rotamers, can be found.

The IR spectra were recorded in ATR instruments, and the main absorption bands are expressed in cm^{-1} .

High-resolution mass spectrometry analyses (HRMS) were performed with electrospray ionisation.

Elemental C and H analyses were performed at the Centres Científics i Tecnològics (CCiT) of the Universitat de Barcelona.

The diffraction experiments were performed at the Universitat de Barcelona, collected on a Bruker APEX II QUAZAR diffractometer equipped with a microfocus multilayer monochromator.

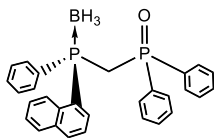
6.3. CHIRAL, PARTIAL AND SELECTIVELY MONO-OXIDIZED DIPHOSPHINE LIGANDS

6.3.1. L2POa

Method A: **BH₃-Pa** (132 mg, 0.5 mmol) was dissolved in 10 mL of tetrahydrofuran and cooled down to 0 °C. Afterwards, 1.6 M *n*-BuLi (0.5 mL, ~0.5 mmol) was added with a syringe and the solution was stirred for 30 minutes. Then, the reaction mixture was allowed to warm up to room temperature and stirred for 1:30 h. After that time, the organolithium solution was cooled down to -78 °C and chlorodiphenylphosphine (92 µL, 1.194 g mL⁻¹, ~0.5 mmol) was then added. The mixture was left stirring overnight. The partial oxidation was carried out with hydrogen peroxide (0.5 mL, 30% w/v, 4.41 mmol) and the reaction mixture was stirred for 1 h. Next, 5 mL of water were carefully added and, subsequently, tetrahydrofuran was removed under vacuum. The product was extracted with dichloromethane (3 x 10 mL), and the combined organic phase was washed with water, dried over anhydrous Na₂SO₄ and filtered. The solvent was removed under reduced pressure, leaving a colourless pasty solid, which was purified by recrystallisation from ethyl acetate and hexane, filtered and finally washed with pentane. **L2POa** was obtained as a white solid. Yield 93 mg (41 %).

Method B: **L2POa** was obtained by a quite similar procedure to the one described above, *method A*, starting from **BH₃-Pa** (132 mg, 0.5 mmol) and with 1.6 M *n*-BuLi (0.5 mL, ~0.5 mmol), but using the already oxidized reagent chlorodiphenylphosphine oxide (95 µL, 1.24 g mL⁻¹, ~0.5 mmol). The oxidation by hydrogen peroxide step was skipped. After the workup, **L2POa** was obtained as a white solid. Yield 125 mg (56 %).

The results of the two methods were quite similar. The low yield and the impurity of the solids obtained in the different experiments carried out did not allow the full characterisation of the product.



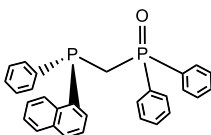
White solid. ³¹P{¹H} NMR (CDCl₃, 101 MHz): δ 23.8 (d, P=O, *J* = 14.1 Hz), 15.5 (bb, P*-BH₃). ¹H NMR (CDCl₃, 400 MHz): δ 8.49 (m, 1H, Ar), 8.22 (s, 1H, Ar), 7.96 (d, *J* = Hz, 2H, Ar), 7.82-7.24 (m, 20H, Ar), 3.64-3.44 (m, 2H, CH₂). HRMS (ESI): *m/z* calc. for C₂₉H₂₈BOP₂ [M+H]⁺ 465.1708; found 465.1713.

6.3.2. L2POa'

Two different methodologies were simultaneously carried out to deprotect the P*P(O) ligands previously obtained. **L2POa** (~0.46 mmol) was dissolved in 10 mL of dichloromethane and the resulting solution was divided in two equal volume fractions. The solvent was removed under vacuum in both Schlenks.

Method A: In one of the volume fractions, **L2POa** (~0.23 mmol) was dissolved in 5 mL of morpholine (5.05 g, 99%+, ~58 mmol) and the solution was left stirred overnight. A colourless solution containing **L2POa'** was obtained.

Method B: In the remaining aliquot, **L2POa** (~0.23 mmol) was treated with HBF₄·Et₂O (157 μ L, 1.19 g mL⁻¹, ~1.15 mmol) and the reaction mixture was left stirred for 1 h. After that time, a degassed saturated solution of NaHCO₃ (10 mL) was added until the solution was basic. The aqueous solution was extracted with dichloromethane (3 x 10 mL), dried over anhydrous Na₂SO₄ and filtered. A colourless solution containing **L2POa'** was obtained.

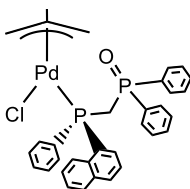


Colourless pasty solid. ³¹P{¹H} NMR (C₆D₆, 101 MHz): δ 25.3 (d, P=O, J = 53.5 Hz), -37.1 (d, P*, J = 53.5 Hz). ¹H NMR (C₆D₆, 400 MHz): δ 8.77-8.73 (m, 1H, Ar), 8.57-8.53 (m, 1H, Ar), 7.98-7.93 (m, 2H, Ar), 7.79-7.74 (m, 1H, Ar), 7.72-7.67 (m, 1H, Ar), 7.63-7.54 (m, 4H, Ar), 7.41-7.34 (m, 2H, Ar), 7.23-7.17 (m, 3H, Ar), 7.06-6.94 (m, 10H, Ar), 2.80 (d, J = 2.78 Hz, 1H, CH₂), 2.80 (d, J = 2.78 Hz, 1H, CH₂), 2.76 (d, J = 2.77 Hz, 1H, CH₂).

6.4. SYNTHESIS OF PALLADIUM COMPLEXES CONTAINING THE L2POa' LIGAND

6.4.1. Pda

L2POa' (~0.23 mmol) obtained from the aliquot deprotected by *Method B*, was dissolved in 10 mL of dichloromethane. Afterwards, **D0** (20 mg, ~0.08 mmol) was added and the suspension was stirred for 1 h. Then, the solvent was removed under reduced pressure, obtaining **Pda**'s crude as a colourless pasty solid.



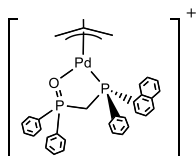
Colourless pasty solid. ³¹P{¹H} NMR (CDCl₃, 101 MHz): δ 25.5 (d, P=O, J = 3.9 Hz, M), 24.7 (d, P=O, J = 8.5 Hz, m), 8.42 (d, P*, J = 3.9 Hz, m), 8.38 (d, P*, J = 8.5 Hz, M). ¹H NMR (CDCl₃, 400 MHz): δ 8.63-8.58 (m, 1H, Ar), 8.39-8.31 (m, 1H, Ar), 8.04 (t, J = 6.68 Hz, 1H, Ar), 7.96-7.66 (m, 8H, Ar), 7.54-7.23 (m, 12H, Ar), 3.99 (m, 2H, CH₂), 2.22 (m, 4H, CH₂), 1.72 (m, 3H, CH₃).

6.4.3. PdOa

Pda (~0.23 mmol) was dissolved in 10 mL of dichloromethane and the resulting solution was divided in two equal volume fractions.

Method A: In one of the aliquots of **Pda** (~0.12 mmol), NH_4PF_6 (132 mg, ~0.8 mmol) was added. The solution was left under intense stirring overnight protected from light. The organic phase was extracted with water to remove any NH_4PF_6 excess and the combined organic phase was washed with water, dried over anhydrous Na_2SO_4 and then, filtered. The solvent was removed under reduced pressure, obtaining **PdOa**'s crude as a pale yellow solid.

Method B: In the remaining volume fraction of **Pda** (~0.12 mmol), TIPF_6 (51 mg, 97%, ~0.14 mmol) was carefully added. The solution was left under intense stirring overnight protected from light. The organic phase was filtered to eliminate any TiCl_4 excess, and the solvent was removed under reduced pressure. The crude was also obtained as a pale yellow solid.

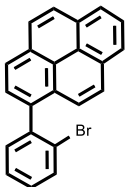


Pale yellow solid. $^3\text{P}\{^1\text{H}\}$ NMR (CDCl_3 , 101 MHz): δ 60.8 (d, $\text{P}=\text{O}$, J = 28.5 Hz, M), 24.7 (d, $\text{P}=\text{O}$, J = 28.5 Hz, m), 17.2 (d, P^* , J = 32.1 Hz, m), 15.5 (d, P^* , J = 30.67 Hz, M). ^1H NMR (CDCl_3 , 400 MHz): δ 8.28-8.26 (d, J = Hz, 1H, Ar), 8.13-8.11 (d, J = Hz, 1H, Ar), 7.96-7.79 (m, 9H, Ar), 7.76-7.30 (m, 15H, Ar), 3.99 (m, 2H, CH_2), 2.14 (s, 2H, CH_2), 2.01 (s, 2H, CH_2), 1.75 (m, 3H, CH_3).

6.5. PREPARATION OF 1-(2-PYRENYL)PHENYL PHOSPHINES

6.5.1. PhPyr-Br

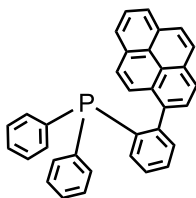
Tris(dibenzylideneacetone)dipalladium(0), $[\text{Pd}_2(\text{dba})_3]$, (343 mg, 375 μmol) and (787 mg, 3 mmol) of triphenylphosphine were dissolved in 80 mL of 1,2-dimethoxyethane to obtain the catalyst, $[\text{Pd}(\text{PPh}_3)_4]$, on-site. The mixture was left stirring for 10 min and 1-bromo-2-iodobenzene (643 μL , 2.2 g mL^{-1} , 5 mmol) was rapidly added. After 15 min of reaction, the mixture had become greenish and a prepared suspension of 1-pyrenyl boronic acid (1.23 g, 5 mmol) in 80 mL of a deoxygenated 2 M aqueous Na_2CO_3 solution was then added. The biphasic mixture was brought to reflux for 12 h at 95 $^\circ\text{C}$. The mixture was cooled down to room temperature and extracted with dichloromethane (2 x 100 mL), and the combined organic phase was washed with water, dried over anhydrous Na_2SO_4 and filtered. The solvents were removed under reduced pressure, leaving a dark brown pasty solid, which was purified by column chromatography (SiO_2 flash, hexane). The solvent was removed under reduced pressure, obtaining **PhPyr-Br** as a white solid. Yield 1.55 g (87 %). The characterisation data matched those reported earlier for this compound.^[11]



White solid. $^1\text{H NMR}$ (CDCl_3 , 400 MHz): δ 8.25 (d, $J = 7.82$ Hz, 1H, Ar), 8.22 (dd, $J^1 = 7.64$ Hz, $J^2 = 0.93$ Hz, 1H, Ar), 8.18 (d, $J = 7.17$ Hz, 1H, Ar), 8.13 (s, 2H, Ar), 8.04 (d, $J = 2.81$ Hz, 1H, Ar), 8.02 (d, $J = 4.36$ Hz, 1H, Ar), 7.91 (d, $J = 7.80$ Hz, 1H, Ar), 7.82 (d, $J = 7.81$ Hz, 1H, Ar), 7.74 (d, $J = 9.19$ Hz, 1H, Ar), 7.50 (s, 1H, Ar), 7.35 (s, 1H, Ar).

6.5.2. PaPhPyr

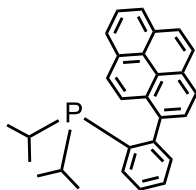
PhPyr-Br (357 mg, 1 mmol) was dissolved in 5 mL of tetrahydrofuran and the resulting solution was cooled to -78 °C. 1.6 M *n*-BuLi in hexane (625 μ L, 1 mmol) was then added using a syringe and the reaction mixture was stirred for 2h. Afterwards, **P-a** (180 μ L, 1 mmol) was added to the organolithium solution. A few hours later, the resulting mixture was allowed to warm up to room temperature. The solution was stirred overnight. After 14 h, deoxygenated water was added, and the solvent was removed under reduced pressure. Still under N₂ atmosphere, the aqueous solution obtained was extracted with dichloromethane (3 x 10 mL), and the combined organic phase was dried over anhydrous Na₂SO₄, then decanted. The solvent was removed under vacuum, obtaining **PaPhPyr** as a yellow solid. Yield 333 mg (72 %).



Yellow solid. ³¹P{¹H} NMR (C₆D₆, 101 MHz): δ -14.0 (s). ¹H NMR (C₆D₆, 400 MHz): δ 8.45 (d, J = 7.91 Hz, 1H, Ar), 8.38 (s, 1H, Ar), 8.25 (d, J = 9.23 Hz, 1H, Ar), 8.04-7.61 (m, 6H, Ar), 7.54-7.44 (m, 1H, Ar), 7.41-7.34 (m, 1H, Ar), 7.32-7.18 (m, 2H, Ar), 7.13-6.87 (m, 6H, Ar). ¹³C{¹H} NMR (CDCl₃, 101 MHz): δ 134.4-124.3 (C, CH, Ar).

6.5.3. PbPhPyr

The procedure used in case of **PaPhPyr** preparation was followed to prepare **PbPhPyr** using **PhPyr-Br** (357 mg, 1 mmol), (625 μ L, 1 mmol) of 1.6 M *n*-BuLi in hexane and (159 μ L, 1 mmol) of **P-b**. The solvent was also removed under vacuum, obtaining **PbPhPyr** as a yellow solid. Yield 264 mg (67 %).

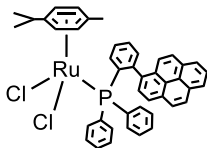


Yellow solid. ³¹P{¹H} NMR (C₆D₆, 101 MHz): δ -4.8 (s). ¹H NMR (C₆D₆, 400 MHz): δ 8.37 (d, J = 9.31 Hz, 1H, Ar), 8.13-8.09 (m, 2H, Ar), 8.07 (s, br, 1H, Ar), 8.05-8.03 (m, 1H, Ar), 8.02-7.99 (m, 2H, Ar), 7.96-7.84 (m, 4H, Ar), 7.69 (dt, J^1 = 5.63, J^2 = 1.82, 1H, Ar), 7.52 (m, 2H, Ar), 7.40 (m, 2H, Ar), 7.28 (s, br, 2H, Ar), 7.17 (m, 2H, Ar), 1.96 (m, 2H, CH), 1.08 (m, 11H, CH₃). ¹³C{¹H} NMR (CDCl₃, 101 MHz): δ 134.3-124.2 (C, CH, Ar), 25.60-24.22 (2CH), 20.87-19.72 (4CH₃).

6.6. SYNTHESIS OF RUTHENIUM COMPLEXES CONTAINING 1-(2-PYRENYL)PHENYL PHOSPHINES

6.6.1. Ru1a

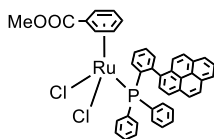
Starting from **PaPhPyr** (~1 mmol) obtained before, 20 mL of dichloromethane were added. The solution was divided in two equal volume fractions in two different Schlenks to prepare both complexes, **Ru1a** and **Ru2a**, simultaneously. In case of **Ru1a**, in one of the volume fractions of **PaPhPyr** (~0.5 mmol), **D1** (115 mg, 0.188 mmol) was added in one of those two fractions mentioned. The solution was stirred for 2 h protected from light. An extraction with dichloromethane (3 x 10 mL) was done to remove any **D1** excess and the combined organic phase was dried over anhydrous Na₂SO₄, then filtered. The solvent was removed under reduced pressure while protected from light, obtaining a bright dark orange foam. The crude was purified by recrystallisation from dichloromethane and hexane, and finally washed with pentane. **Ru1a** was obtained as a dark orange solid. Yield 225 mg (41 %). Single crystals suitable for XRD analysis were obtained by slow diffusion of hexane in a solution of **Ru1a** in dichloromethane at 2-4 °C protected from light.



Dark orange solid. **IR** (ATR): 693.73, 716.52, 723.81, 743.99, 847.78, 1092.18, 1434.88, 1487.52, 1490.22, 1583.25, 2945.36, 3062.19 cm⁻¹. **³¹P{¹H} NMR** (CDCl₃, 101 MHz): δ +24.1 (s). **¹H NMR** (CDCl₃, 400 MHz): δ 9.14 (d, *J* = 8.02 Hz, 1H, Ar), 9.10 (d, *J* = 7.97 Hz, 1H, Ar), 8.13 (d, *J* = 6.94 Hz, 1H, Ar), 8.03-7.90 (m, 2H, Ar), 7.85-7.79 (m, 1H, Ar), 7.85-7.79 (m, 1H, Ar), 7.74-7.68 (m, 1H, Ar), 7.65-7.61 (m, 1H, Ar), 7.59-7.49 (m, 2H, Ar), 7.41-7.30 (m, 2H, Ar), 7.16-7.11 (m, 1H, Ar), 7.02 (d, *J* = 9.2 Hz, 1H, Ar), 6.91 (d, *J* = 7.33 Hz, 1H, Ar), [6.66-6.05] (td, *J*¹ = 7.22 Hz, *J*² = 2.99 Hz, 1H, Ar), [6.53-5.88] (t, *J* = 7.12 Hz, 1H, CH_{Arene}), [5.95-5.33] (d, *J* = 6.26 Hz, 1H, CH_{Arene}), 5.23-5.16 (m, 1H, CH_{Arene}), [4.99-4.60] (m, 1H, CH_{Arene}), 2.93-2.65 (m, 1H, CH), 1.68 (s, 3H, CH₃-C_{Arene}), [1.34-1.02] (d, *J* = 6.95 Hz, 6H, 2CH₃). **¹³C{¹H} NMR** (CDCl₃, 101 MHz): δ 137.5-124.2 (C, CH, Ar), 113.6 (d, *J* = 5.9 Hz, C), 102.7 (C), 87.5 (d, *J* = 3.5, 2C, CH), 88.0 (2CH), 31.9 (CH), 22.7 (br, 2CH₃), 18.7 (CH₃). **HRMS** (ESI): *m/z* calc. for C₄₄H₃₇Cl₂PRu [M-Cl]⁺ 733.1359; found 733.1360. **EA**: calc. for C₄₄H₃₇Cl₂PRu C (68.75 %), H (4.85 %); found C (66.05 %), H (5.52 %).

6.6.2. Ru2a

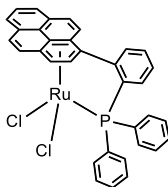
As mentioned above, **Ru2a** was simultaneously prepared to **Ru1a** from a common, divided in two fractions, solution of **PaPhPyr**. In the remaining aliquot of **PaPhPyr** (~0.5 mmol) solution, **D2** (116 mg, 0.188 mmol) was added. The suspension was stirred for 2 h protected from light and then filtered to remove any **D2** excess. The solvent was removed under reduced pressure while protected from light, obtaining a brownish pasty solid. The crude was purified by recrystallisation from dichloromethane and hexane and finally washed with pentane. **Ru2a** was obtained as a light orange solid. Yield 214 mg (39 %).



Light orange solid. **IR** (ATR): 692.95, 723.96, 745.78, 768.39, 833.24, 847.62, 948.52, 1093.20, 1108.95, 1986.32, 1274.07, 1292.73, 1433.33, 1462.89, 1512.03, 1098.87, 1726.53 (C=O), 3057.36 cm^{-1} . **$^{31}\text{P}\{^1\text{H}\}$ NMR** (CDCl_3 , 101 MHz): δ +26.9 (s). **^1H NMR** (CDCl_3 , 400 MHz): δ 8.81 (bb, 2H, Ar), 8.14 (d, J = 7.18 Hz, 1H, Ar), 8.06-7.85 (m, 4H, Ar), 7.81-7.69 (m, 3H, Ar), 7.62 (d, J = 8.55 Hz, 2H, Ar), 7.55-7.36 (m, 6H, Ar), 7.28-7.05 (m, 5H, Ar), [6.47-6.41] (d, J = 6.05 Hz, 2H, CH_{Arene}), [6.31-5.89] (bb, 2H, CH_{Arene}), 6.08 (m, 1H, CH_{Arene}), 5.18 (q, J = 3.85 Hz, 1H, CH_{Arene}), [5.12-5.06] (t, J = 5.80 Hz, 1H, CH_{Arene}), 4.76 (m, 1H, CH_{Arene}), [3.96-3.93] (s, 3H, OCH_3). **$^{13}\text{C}\{^1\text{H}\}$ NMR** (CDCl_3 , 101 MHz): δ 165.2 (C=O), 137.5-124.0 (1C, CH, Ar), 90.9 (3C, CH), 86.3 (1C, CH), 53.3 (C, CH_3). **HRMS** (ESI): m/z calc. for $\text{C}_{42}\text{H}_{35}\text{Cl}_2\text{NO}_2\text{PRu}$ [$\text{M}+\text{NH}_4$] $^+$ 788.0820; found 788.0831. **EA**: calc. for $\text{C}_{42}\text{H}_{31}\text{Cl}_2\text{O}_2\text{PRu}$ C (65.46 %), H (4.05 %); found C (61.79 %), H (4.30 %).

6.6.3. Ru^a'

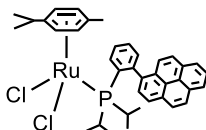
Ru1a and **Ru2a** were both, in two different Schlenks, dissolved in 20 mL of dichloromethane. The solutions were exposed to the light of a common office lamp under stirring. In case of **Ru1a**, it took 4 days to get the total conversion into **Ru^a'**. On the other hand, **Ru2a** was completely converted after 6 h. After that, the solvent was removed under reduced pressure, obtaining in both cases dark brown pasty solids. The crudes were purified by recrystallisation from dichloromethane and hexane and finally washed with pentane. **Ru^a'** was obtained as a dark brown solid. Yield 113 mg (36 %).



Dark brown solid. **IR** (ATR): 609.66, 690.37, 724.11, 742.71, 842.71, 995.66, 1092.65, 1186.22, 1275.39, 1434.39, 1482.08, 1585.99, 1732.60, 1963.47, 3052.84, 3479.90 cm^{-1} . **$^{31}\text{P}\{^1\text{H}\}$ NMR** (CD_2Cl_2 , 101 MHz): δ +63.1 (s). **^1H NMR** (CD_2Cl_2 , 400 MHz): δ 8.62 (d, J = 7.8 Hz, 1H), 8.14-7.16 (m, 16H), [6.64-6.18] (d, J = 9.54 Hz, 2H, CH_{Arene}), [5.54-5.09] (m, 1H, CH_{Arene}). **HRMS** (ESI): m/z calc. for $\text{C}_{34}\text{H}_{23}\text{Cl}_2\text{PRu}$ $[\text{M}-\text{Cl}]^+$ 599.0263; found 599.0262. **EA**: calc. for $\text{C}_{34}\text{H}_{23}\text{Cl}_2\text{PRu}$ C (64.36 %), H (3.65 %); found C (53.70 %), H (3.62 %).

6.6.4. Ru1b

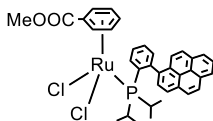
The procedure carried out to prepare **Ru1b** and **Ru2b**, also simultaneously synthesized as **Ru1a** and **Ru2a**, was the same mentioned above in case of **Ru1a** and **Ru2a** but starting from **PbPhPyr** (~1 mmol). For the preparation of **Ru1b**, in one of the aliquots of the solution of **PbPhPyr** (~0.5 mmol) was added **D1** (115 mg, 0.188 mmol). Finally, after the workup, **Ru1b** was obtained as a dark orange solid. Yield 118 mg (25 %).



Dark orange solid. **IR** (ATR): 632.14, 696.06, 727.40, 743.78, 799.43, 850.63, 885.86, 999.69, 1030.54, 1057.32, 1091.90, 1158.33, 1188.32, 1279.18, 1326.12, 1386.35, 1434.71, 1468.96, 1481.35, 1584.70, 2869.19, 2928.97, 2958.86, 3048.08 cm^{-1} . **$^{31}\text{P}\{^1\text{H}\}$ NMR** (CDCl_3 , 101 MHz): δ +24.1 (s). **^1H NMR** (CDCl_3 , 400 MHz): δ 8.71 (bb, 1H, Ar), 8.30-7.89 (m, 4H, Ar), 7.86-7.80 (m, 4H, Ar), 7.65-7.56 (m, 1H, Ar), 7.41-7.33 (m, 5H, Ar), [5.94-5.76] (d, J = 6.37 Hz, 1H), 5.47 (d, J = 5.98 Hz, 2H, CH_{Arene}), 5.34 (d, J = 5.98 Hz, 2H, CH_{Arene}), 5.19 (d, J = 8.18 Hz, 2H, CH_{Arene}), 4.98 (dd, J^1 = 6.13 Hz, J^2 = 1.02 Hz, 2H, CH_{Arene}), 2.96-2.82 (m, 2H, CH), 2.16 (s, 6H, $\text{CH}_3\text{-C}_{\text{Arene}}$), 1.28 (d, J = 6.94 Hz, 6H, CH_3), 1.10 (d, J = 6.97 Hz, 6H, CH_3). **$^{13}\text{C}\{^1\text{H}\}$ NMR** (CDCl_3 , 101 MHz): δ 135.1-127.8 (C, CH, Ar), 92.8-88.3 (7CH), 33.4 (CH), 25.8 (bb, 2 CH_3), 21.8 (bb, CH_3), 20.2 (bb, CH_3), 19.6 (bb, CH_3), 22.3 (CH_3), 20.3 (bb, CH_3). **HRMS** (ESI): m/z calc. for $\text{C}_{28}\text{H}_{29}\text{Cl}_2\text{PRu}$ $[\text{M-Arene-Cl}+2\text{H}]^+$ 533.0733; found 533.0734. **EA**: calc. for $\text{C}_{38}\text{H}_{41}\text{Cl}_2\text{PRu}$ C (65.14 %), H (5.90 %); found C (58.91 %), H (5.93 %).

6.6.5. Ru2b

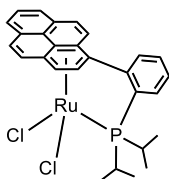
As mentioned above, **Ru2b** was prepared simultaneously to **Ru1b** following the same procedure as in case of **Ru1a** and **Ru2a**. In the remaining aliquot of **PbPhPyr** (~0.5 mmol) solution, **D2** (116 mg, 0.188 mmol) was added. When workup was finished, **Ru2b** was obtained as a light orange solid. Yield 167 mg (35 %).



Light orange solid. **IR** (ATR): 618.51, 643.48, 672.45, 695.64, 726.50, 768.22, 819.10, 847.85, 692.59, 998.72, 1036.58, 1093.56, 1108.26, 1143.84, 1189.47, 1272.22, 1291.68, 1433.21, 1522.07, 1724.40 (C=O), 2870.03, 2929.10, 2955.36, 3055.51 cm^{-1} . **$^3\text{P}\{^1\text{H}\}$ NMR** (CDCl_3 , 101 MHz): δ +50.6 (s). **^1H NMR** (CDCl_3 , 400 MHz): δ 8.31-8.12 (m, 2H, Ar), 8.07-8.03 (m, 1H, Ar), 7.92 (d, J = 9.14 Hz, 1H, Ar), 7.77-7.69 (m, 3H, Ar), 7.46-7.36 (m, 5H, Ar), [6.65-6.33] (d, J = 6.59 Hz, 3H, CH_{Arene}), 5.37-5.32 (m, 1H, CH_{Arene}), 5.08 (t, J = 6.77 Hz, 1H, CH_{Arene}), [4.00-3.96] (s, 3H, OCH_3), 1.65 (bb, 2H, CH), 1.50-1.00 (m, 6H, CH_3). **$^{13}\text{C}\{^1\text{H}\}$ NMR** (CDCl_3 , 101 MHz): δ 164.4 (C=O), 133.4-123.7 (C, CH, Ar), 93.6 (CH), 93.2 (CH), 90.3 (CH), 89.0 (d, J = 9.2 Hz, C), 86.7 (CH), 85.6 (CH), 53.7 (CH_3), 30.3 (d, J = 23.7 Hz, CH), 30.4 (d, J = 25.3 Hz, CH), 23.2 (CH_3), 20.1 (d, J = 6.0 Hz, CH_3), 19.8 (d, J = 6.2 Hz, CH_3), 18.3 (CH_3). **HRMS** (ESI): m/z calc. for $\text{C}_{36}\text{H}_{39}\text{Cl}_2\text{NO}_2\text{PRu}$ [$\text{M}+\text{NH}_4$] $^+$ 720.1132; found 720.1133. **EA**: calc. for $\text{C}_{36}\text{H}_{35}\text{Cl}_2\text{O}_2\text{PRu}$ C (61.54 %), H (5.02 %); found C (57.93 %), H (5.00 %).

6.6.6. Rub'

Ru1b and **Ru2b** were both, in two different Schlenks, dissolved in 20 mL of dichloromethane. The solutions were exposed to the light of a common office lamp under stirring. In case of **Ru1b**, it took 4 days to achieve the total conversion into **Rub'**. On the other hand, **Ru2b** was completely converted after 6 h. After that, the solvent was removed under reduced pressure, obtaining in both cases dark brown pasty solids. The crudes were purified by recrystallisation from dichloromethane and hexane and finally washed with pentane. **Rub'** was obtained as a dark green solid. Yield 80 mg (20 %). Single crystals suitable for XRD analysis were obtained by slow diffusion of hexane in a solution of **Rub'** in dichloromethane at 2-4 °C.



Dark green solid. **IR** (ATR): 667.93, 675.99, 753.24, 796.29, 863.61, 882.20, 1036.45, 1093.53, 1109.45, 1274.92, 1434.71, 1458.87, 1731.86, 2063.83, 2234.87, 2867.00, 2920.24, 2953.51, 2973.47, 3051.35 cm^{-1} . **$^3\text{P}\{^1\text{H}\}$ NMR** (CD_2Cl_2 , 101 MHz): δ +82.5 (s). **^1H NMR** (CD_2Cl_2 , 400 MHz): δ 8.07-7.38 (m, 8H, Ar), 6.68-6.36 (m, 2H, CH_{Arene}), 1.51-1.17 (m, 9H, CH, CH_3). **HRMS** (ESI): m/z calc. for $\text{C}_{28}\text{H}_{27}\text{ClIPRu}$ [$\text{M}-\text{Cl}$] $^+$ 531.0582; found 531.0580. **EA**: calc. for $\text{C}_{28}\text{H}_{27}\text{Cl}_2\text{PRu}$ C (59.37 %), H (4.80 %); found C (54.47 %), H (5.01 %).

7. CONCLUSIONS

- The two synthetic methods explored to synthesize the P*P(O) ligands worked but they will have to be optimised in order to obtain the pure products in greater yields.
- Using $\text{HBF}_4 \cdot \text{Et}_2\text{O}$ complex to deprotect the P*P(O) ligands is a good strategy, since the deprotection was complete and the product could be obtained, not as in case of using morpholine.
- The two isomers of **Pda** complex were easily prepared by the splitting of **D0** with **L2POa'**.
- The two isomers of **Pda** resulted in also two isomers of **PdOa** chelated complex using TIPF_6 as halide scavenger. **L2POa'** is able to act, as expected, as a bidentate ligand.
- All the ruthenium complexes were successfully obtained by the splitting of **D1** and **D2** with **PaPhPyr** and **PbPhPyr**.
- The expected tethered ruthenium complexes, **Rua'** and **Rub'**, could be photochemically obtained under mild conditions by the arene decoordination. The reaction rate is higher when the arene is an electron-deficient one.
- It seems the ^{31}P signals of the ruthenium complexes are so broad they can not be observed with low resolution instruments.

8. REFERENCES AND NOTES

1. Jugé, S.; Stephan, M.; Laffitte, J. A.; Genêt, J. P. *Tetrahedron Lett.* **1990**, 31, 6357-6360.
2. Grabulosa, A.; Granell, J.; Muller, G. *Coord. Chem. Rev.* **2007**, 251, 25-90.
3. (a) Basiouny, M. M. I.; Schmidt, J. A. R., *Organometallics* **2017**, 36, 721-729. (b) Hosseinnajad, T.; Kazemi, T., *Radiochim.*, **2016**, 104(2), 97-105.; (c) Pavankumar, B. B. *et al.*, *RSC Adv.*, **2015**, 5, 4727.
4. Faller, J. W.; Parr, J., *Organometallics* **2000**, 19, 1829-1832.
5. Garrou, P. E., *Chem. Rev.*, **1981**, 81, 229-266.
6. Brissos, R. F.; Clavero, P.; Gallen, A.; Grabulosa, A.; Muller, G.; Gámez, P.; *Inorg. Chem.* **2018**, 57, 14786-14797.
7. (a) Romero-Canelón, I.; Salassa, L.; Sadler, P. J., *J. Med. Chem.* **2013**, 56, 1291-1300; (b) Rafter, E.; Gilheany Declan, G.; Reek Joost, N. H.; van Leeuwen, P. W. N. M., *ChemCatChem* **2010**, 2, 387-391.
8. (a) Aznar, R.; Grabulosa, A.; Mannu, A.; Muller, G.; Sainz, D.; Moreno, V.; Font-Bardia, M.; Calvet, T.; Lorenzo, J., *Organometallics* **2013**, 32, 2344-2362; (b) Navarro, M.; Vidal, D.; Clavero, P.; Grabulosa, A.; Muller, G., *Organometallics* **2015**, 34, 973-994; (c) Grabulosa, A.; Mannu, A.; Mezzetti, A.; Muller, G., *J. Organomet. Chem.* **2012**, 696, 4221-4228.
9. (a) Grabulosa, A.; Muller, G.; Ceder, R.; Maestro, M. A. *Eur. J. Inorg. Chem.* **2010**, 3372-3383; (b) Grabulosa, A.; Muller, G.; Ordinas, J. I.; Mezzetti, A.; Maestro, M. A.; FontBardia, M.; Solans, X. *Organometallics* **2005**, 24, 4961-4973.
10. Clavero, P.; Grabulosa, A.; Font-Bardia, M.; Muller, G., *J. Mol. Catal. A: Chem.* **2014**, 391, 183-190.
11. Lamale, B.; Henry, W. P.; Daniels, L. M.; Zhang, C.; Klein, S. M.; Jiang, Y. L., *Tetrahedron* **2009**, 65, 62-69.

9. ACRONYMS

IR: Infrared spectroscopy

NMR: Nuclear Magnetic Resonance

gHSQC: gradient Heteronuclear Single Quantum Coherence spectroscopy

HRMS: High Resolution Mass Spectroscopy

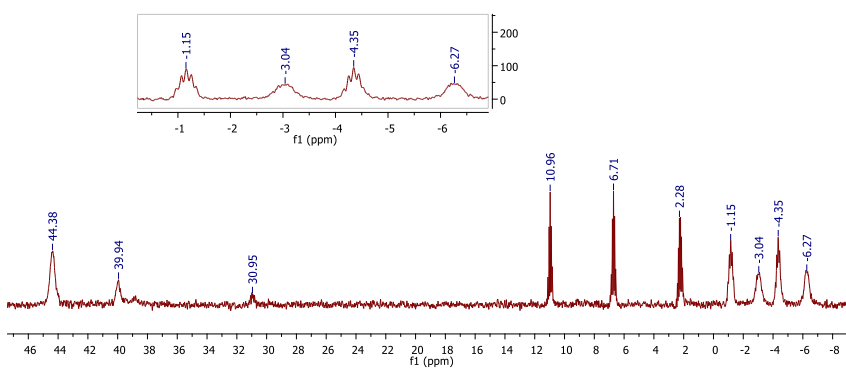
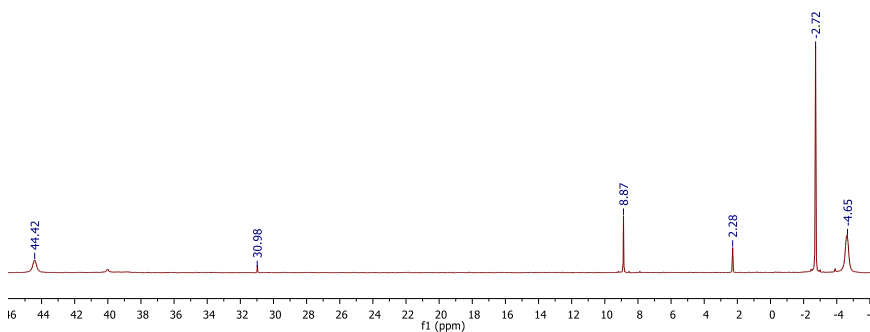
EA: Elemental Analysis

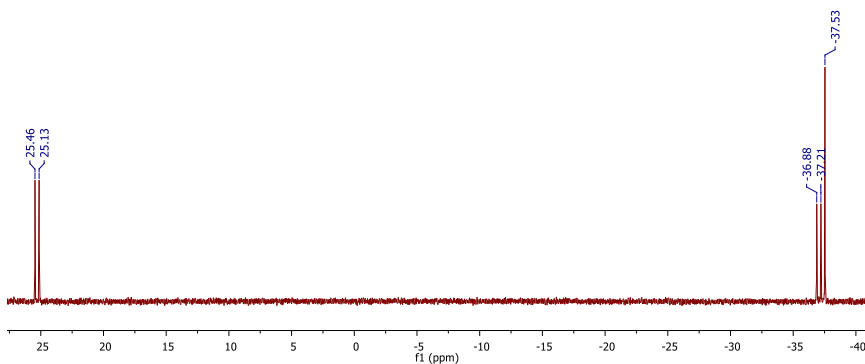
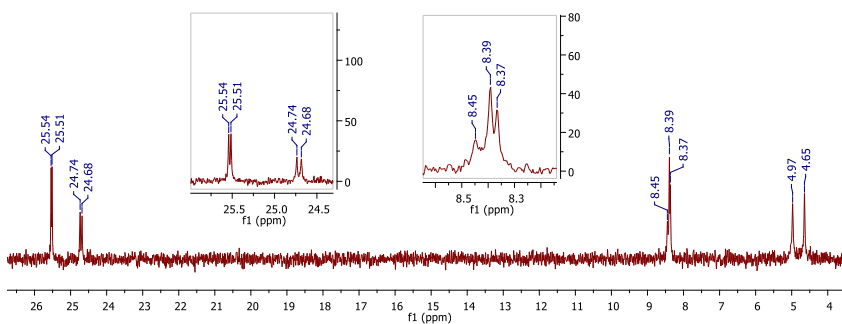
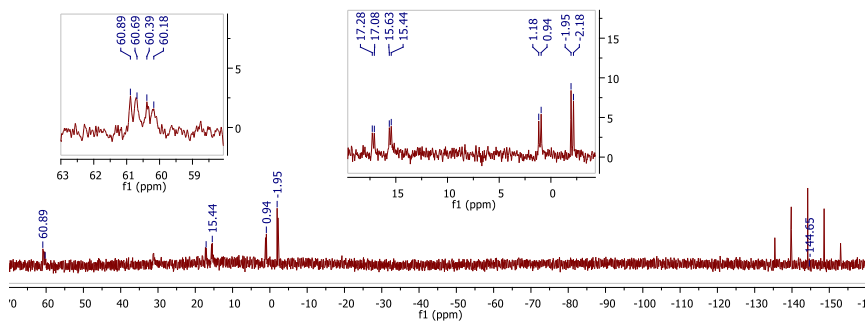
XRD: X-Ray Diffraction

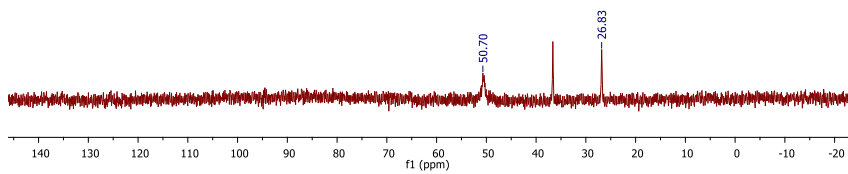
ATR: Attenuated Total Reflection

APPENDICES

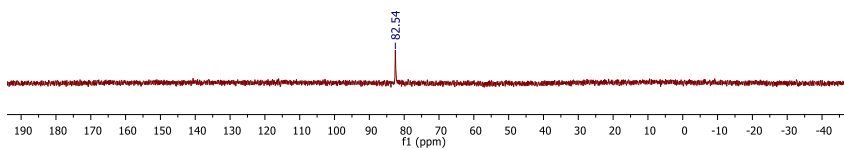
APPENDIX 1: NMR SPECTRA



3. $^{31}\text{P}\{^1\text{H}\}$ NMR spectrum of L2POa'.4. $^{31}\text{P}\{^1\text{H}\}$ NMR spectrum of Pda.5. $^{31}\text{P}\{^1\text{H}\}$ NMR spectrum of PdOa.



6. $^{31}\text{P}\{^1\text{H}\}$ NMR spectrum of **Ru2b**.



7. $^{31}\text{P}\{^1\text{H}\}$ NMR spectrum of **Rub'**.

